

SPACE RESEARCH COORDINATION CENTER



**GAS PHASE RECOMBINATION
OF HYDROGEN AND DEUTERIUM**

BY

**CASE FILE
COPY**

**DANIEL W. TRAINOR, DAVID O. HAM,
AND FREDERICK KAUFMAN**

SRCC REPORT NO. 186

**UNIVERSITY OF PITTSBURGH
PITTSBURGH, PENNSYLVANIA**

MARCH 1973

The Space Research Coordination Center, established in May, 1963, has the following functions: (1) it administers predoctoral and postdoctoral fellowships in space-related science and engineering programs; (2) it makes available, on application and after review, allocations to assist new faculty members in the Division of the Natural Sciences and the School of Engineering to initiate research programs or to permit established faculty members to do preliminary work on research ideas of a novel character; (3) in the Division of the Natural Sciences it makes an annual allocation of funds to the Interdisciplinary Laboratory for Atmospheric and Space Sciences; (4) in the School of Engineering it makes a similar allocation of funds to the Department of Metallurgical and Materials Engineering and to the program in Engineering Systems Management of the Department of Industrial Engineering; and (5) in concert with the University's Knowledge Availability Systems Center, it seeks to assist in the orderly transfer of new space-generated knowledge in industrial application. The Center also issues periodic reports of space-oriented research and a comprehensive annual report.

The Center is supported by an Institutional Grant (NsG-416) from the National Aeronautics and Space Administration, strongly supplemented by grants from the A. W. Mellon Educational and Charitable Trust, the Maurice Falk Medical Fund, the Richard King Mellon Foundation and the Sarah Mellon Scaife Foundation. Much of the work described in SRCC reports is financed by other grants, made to individual faculty members.

Gas Phase Recombination of Hydrogen and Deuterium Atoms*

Daniel W. Trainor[†], David O. Ham^{††}, and Frederick Kaufman

Department of Chemistry, University of Pittsburgh

Pittsburgh, Pennsylvania 15213

ABSTRACT

Rate constants for the reaction $H + H + M \rightarrow H_2 + M$, with $M = H_2$, He, and Ar were measured over the temperature range 77 to 298°K. Hydrogen atoms were produced by thermal dissociation and absolute atom concentrations were measured through use of self-balancing, isothermal catalytic probe detector. The specific rate constants were $8.1 \pm 0.4 \times 10^{-33}$, $7.0 \pm 0.4 \times 10^{-33}$, and $9.2 \pm 0.6 \times 10^{-33} \text{ cm}^6 \text{ molecules}^{-2} \text{ sec}^{-1}$ at 298°K for $M = H_2$, He, and Ar respectively; these values rising to $18.5 \pm 2.2 \times 10^{-33}$, $12.0 \pm 1.5 \times 10^{-33}$, and $27.4 \pm 4.6 \times 10^{-33} \text{ cm}^6 \text{ molecules}^{-2} \text{ sec}^{-1}$ at 77°K. For the equivalent deuterium atom process with D_2 as the third body, the rate constants are $6.1 \pm 0.3 \times 10^{-33} \text{ cm}^6 \text{ molecules}^{-2} \text{ sec}^{-1}$ at 298°K and $15.1 \pm 1.0 \times 10^{-33} \text{ cm}^6 \text{ molecules}^{-2} \text{ sec}^{-1}$ at 77°K. These values are compared with previous experimental measurements and with recent theoretical calculations.

MARCH 1973

I. Introduction

As the simplest termolecular reaction and one that is well suited for rigorous calculations, the gas phase recombination of hydrogen atoms in the presence of third body atoms or molecules, M, continues to generate wide interest both theoretically and experimentally. Although there have been many experimental determinations of the hydrogen atom recombination rate constant¹⁻¹⁶ ranging from the earliest investigation by Smallwood¹ in 1929, to recent studies of Larkin and Thrush,¹⁰⁻¹¹ and of Bennett and Blackmore,¹²⁻¹⁴ its value has remained surprisingly uncertain, there is very little known about its temperature dependence, particularly below room temperature, and about the effectiveness of different M. Recent room temperature studies for M = H₂, since 1960, show poor agreement as they report specific rate constants ($\frac{d[H_2]}{dt} / [H]^2 [M]$) covering a range from 3.6 to 200 x 10⁻³³ cm⁶ molecule⁻² sec⁻¹. A critical review of these data, as well as those obtained in flames and shock tubes, can be found in a new book by Baulch, Drysdale, Lloyd, and Horne.¹⁷

Aside from its continuing challenge to the experimentalist and the extreme dearth of measurements of the temperature dependence and of the M effect, the problem has become much more interesting due to the recent calculations of a quantum mechanical orbiting resonance theory by Roberts, Bernstein and Curtiss,¹⁸ and a classical phase space theory by Shui, Appleton and Keck.^{19,20} These theories predict quite different behavior in the low temperature region, and thus have stimulated much interest in experimental studies covering a wide temperature range for a variety of third bodies.

In this paper, we report rate constants for the reaction measured

in a flow system over the temperature range 77 to 298°K, and for M = H₂, He, and Ar. As the reaction is second order in H, the absolute H-atom concentration must be measured accurately. In addition, experimental conditions should be selected so as to provide a manageable kinetic model for treating the data. For these measurements, an isothermal catalytic probe atom detector was utilized as the absolute atom measuring device. Its accuracy as an atom detector is dependent, however, both on complete atom recombination occurring on the probe and on quantitative energy accommodation of the heat released on recombination. We have measured the efficiency of our probe for both these effects and found it to be complete. The present data thus represent the first extensive and self-consistent experimental study of the temperature, isotope, and M-effect at and below 300°K and can form the basis for fruitful comparison with theory.

II. Experimental

A. Flow System

The apparatus is shown schematically in Fig. 1. Gaseous reactants are admitted through needle valves upstream of the reaction tube and their flowrates are measured by float type flowmeters (Fisher and Porter) calibrated with a volumetric displacement device (Vol-u-meter, G. K. Porter Co.). Calibrations were reproducible to $\pm 2\%$ over a period of two years. The reaction tube pressure is measured with a pressure transducer (Validyne Engineering Co., Model DP7, ± 1 psi and Model CD12 Indicator) calibrated with a McLeod gauge (Consolidated Vacuum, Model GM-100A) and oil manometer.

The central 100cm of the quartz reaction tube (1.000 inch i.d., total length 180 cm) is surrounded by a copper cooling jacket which, in turn, is surrounded by a cylindrical heating mantle, consisting of a long central section and two separate end sections, controlled by a solid state

temperature controller (RI controls, thermal Model MPRY). The accessible temperature range is 77 to about 900°K, but the present work covers only the lower range, 77 to 298°K. These lower temperatures are obtained by passing cold N₂ through the copper jacket, the gas temperature being measured by three external thermocouples (iron-constantan) placed between the reaction tube and the cooling jacket, and by the probe itself calibrated and used as a resistance thermometer. For experiments at 77°K, liquid N₂ is blown through the cooling jacket from a large (160 lit) container and collected in small dewar flasks at the exit ports. For experiments at temperatures between 77 and 296°K, liquid N₂ is pumped through the jacket by suction using a small rotary air pump (Eberbach Corp.) at controlled flow rates.

B. H-Atom Source

Hydrogen atoms are produced by the thermal dissociation of H₂ (99.999% pure) on a hot tungsten filament which is suspended in a water cooled quartz housing as shown in Fig. 2. H₂ is passed through a liquid nitrogen cooled zeolite trap (molecular sieve, 5Å, Davison Chemical), through the upstream dissociator, then through a liquid nitrogen cooled glass wool trap, before passing over the second dissociator and through a pyrex to quartz seal 14 cm long and 1.2 cm i.d. into the main flow tube. The tungsten filaments were prepared by tightly winding 0.015 inch wire on a mandril and then stretching it into a loosely wound helix about 30-40 cm long. This wire was spot-welded to lead-in rods which are part of a demountable O-ring glass joint. This makes it possible to move either dissociator from one position to the other. Initially, a filament was placed in the upstream position where it was heated to approximately 2200°K in a continuous flow of H₂ for a period of several hours. After this treatment, it is ready for use as the atom source in the downstream position and another W-wire

assembly is placed in the upstream position. This assures the instant availability of a properly pretreated W-filament, and also removes from the gas stream any reducible impurity by reaction with H or H₂ at high temperatures followed by condensation in the packed trap at 77°K.

C. H-Atom Detector

The isothermal probe atom detector was constructed of 63 cm of Pt/10%Rh thermocouple wire (0.010 inch diameter, Engelhard Industries) which was wound as a spiral on a quartz probe support as shown in Fig. 3. The probe wire forms one arm of self-balancing Kelvin bridge whose circuit diagram is shown in Fig. 4. A Kelvin rather than Wheatstone bridge network is used in order to eliminate or greatly reduce the effect of lead and contact resistance. This is particularly advantageous under present experimental conditions where variable lengths of the copper lead wires are at low temperatures and would therefore contribute a changing resistance due to their temperature coefficients.

In normal operation of the self-balancing bridge, the standard resistor (0 to 1 ohm, 0.1 ohm steps) is set at a resistance, R_S , which equals that of the probe, R_D , at a sufficiently elevated temperature, $\Delta T \leq 100^\circ\text{C}$, such that the maximum temperature rise due to atom recombination is less than (but not too much less than) ΔT . The bridge unbalance signal, $R_S - R_D$, is amplified by the operational amplifier (Philbrick, P85A, gain - 2000) and controls the current passed by the transistor (NPN silicon power transistor, 2N2230). In this manner, since the probe resistance, R_D , increases with increasing current (temperature) whereas R_S is independent of it, a feedback loop is established which keeps the magnitude of $R_S - R_D$ at less than about 0.001 ohm, corresponding to an uncertainty of less than 0.25°C in the temperature of the probe wire.

The probe is completely enclosed in the flow system (see Fig. 1), the wires to the Kelvin bridge passing through a vacuum feedthrough. Attached to the end of the probe support rod is a small steel cylinder, which is surrounded by a solenoid. When the solenoid is activated, the probe is thereby magnetically coupled to the external drive mechanism, causing the probe to move up-or downstream in the flow tube over a distance of 1 meter at any one of ten steady speeds from 0.05 to 2.3 cm sec⁻¹ selected by appropriate speed reduction of a synchronous motor (Apcor speed reducer, Model 2405 coupled to a Bodine Motor, 1/15 HP, 690 R.P.M., 115 V ac 60 CPS). This arrangement of the probe lead wires inside a narrow, evacuated tube eliminates the need for sliding rods and O-ring seals. The main gas flow passes through the pumping port at the end of the reaction zone, and the effect of the additional gas flow path on conditions in the reaction zone is negligible.

Cylinder gases of the following indicated purity were used without further purification: H₂ (ultrahigh purity, 99.999%), D₂ (C.P., 99.5%), He (high purity, 99.995%), Ar (prepurified, 99.998%). NO (technical, 98.5%) and NO Cl (97%) were condensed, pumped and distilled several times before use.

III. Calibrations and Procedures.

Catalytic probe atom detectors²¹ have been criticized as unreliable for accurate kinetic work because of their lack of specificity, possible inefficiency at collecting and/or detecting atoms, and perturbation of the system by acting as an atom sink and thereby producing concentration gradients near the probe. Moreover, the general limitations of flow system parameters must be kept in mind and checked experimentally. Gaseous impurities were minimized through use of a helium leak tight flow system and ultra pure hydrogen. It was further necessary to test whether the probe

- (a) intercepted and recombined the H-atoms quantitatively; and
- (b) received their total recombination energy, i.e. exhibited unit energy accommodation.

A. Atom Collection Efficiency

To measure the efficiency of the probe as an atom collector, several experiments were performed using the set-up shown in Fig. 5. With the probe inserted upstream of the H-atom entrance port and placed at position A in the main flow tube, addition of small amounts of NO to the atom stream permitted measurement of the resulting HNO^* chemiluminescence emission intensity, I , by the photocurrent of a photomultiplier tube (RCA 7265, S-20 response) viewing the flow tube through an interference filter (IR Industries) which had a transmission maximum at 6925 \AA and a bandwidth (fwhm) of 100 \AA . Since $I = I_0[\text{H}][\text{NO}]$,²² the intensity measures relative H-atom concentrations when $[\text{NO}]$ is held constant. The probe was then moved downstream past the H-atom source inlet to position B and the HNO^* intensity was re-determined. Experiments indicated that the fraction of H-atoms which were not removed by the probe increased from 1 to 5% as the linear flow velocity was increased from 500 to 1700 cm sec^{-1} . Since kinetic data were collected mainly at velocities near 500 cm sec^{-1} , the probe is thus about 99% efficient in recombining H-atoms.

B. Energy Accommodation

The energy accommodation at the detector, i.e. the question whether the difference in electrical power between atoms off and on as measured by the Kelvin bridge can be set equal to the power due to the full recombination of the H-atom flow, was tested by comparison with H + NOCl titrations.²³ Here the quantitative, fast reaction $\text{H} + \text{NOCl} \rightarrow \text{HCl} + \text{NO}$ removes H and makes NO, so that the intensity of the red HNO^* emission first rises and then decreases to zero with increasing NOCl additions. The concentration of NOCl added at the end point, when the glow is barely extinguished, is exactly

equal to the H-atom concentration if the titration reaction is considered infinitely fast. As long as H is in excess, $I = I_0[H][NO] = I_0[H][NOCl]_{\text{added}}$ and $[H] + [NOCl]_{\text{added}} = [H]_0$, the original H-atom concentration to be determined. Rearranging, we obtain $\frac{I}{I_0[NOCl]_{\text{added}}} = [H]_0 - [NOCl]_{\text{added}}$ and a plot of $\frac{I}{[NOCl]_{\text{added}}}$ vs. $[NOCl]_{\text{added}}$ should be linear and have an x-axis intercept at which $[NOCl]_{\text{added}}$ equals $[H]_0$ as is shown in Fig. 6. These titration plots have large probable errors for several reasons such as the difficulty of controlling and measuring pressures and flows of highly corrosive NOCl and extrapolation to zero $\frac{I}{[NOCl]_{\text{added}}}$. For each of the 10 experiments listed in Table 1, $[H]$ was measured independently by the catalytic probe method and by NOCl titration, with the result that $[H]_{\text{probe}} = (0.99 \pm 0.08) [H]_0$, showing that energy accommodation at the probe is quantitative and ruling out the possibility that vibrationally excited H_2 may be formed at the catalytic surface and carried downstream unrelaxed.

C. Flow Characteristics

Calculation of kinetic rate constants from measurements of absolute atom concentrations as a function of distance along the flow tube requires an understanding of the flow parameters, of the perturbation introduced by the probe, and of all other simultaneous atom loss processes, particularly of the rate of wall recombination. For the first of these three problems, the characterization of the flow, one needs to justify the use of the simple one-dimensional plug flow approximation by showing that the viscous pressure drop, radial, and axial diffusion effects are all negligible. Under typical conditions such as pressure ~ 6 torr, $\bar{v} \sim 500$ cm/sec, the measured (and calculated) pressure drop was $< 1\%$. Radial concentration gradients were estimated by the relation $\Delta c/c \sim r_0^2 (k_V + 3k_W)/8D$, where k_V and k_W are effective first-order constants for volume and wall removal of atoms and D is the diffusion coefficient.²⁴ Typically, $\Delta c/c$ was calculated to be about 1% showing this

effect to be negligible, too. Axial diffusion leads in a one-dimensional approximation to an underestimate of the true, effective first-order rate constant such that $k^I = k_{\text{obs}}^I (1 + k_{\text{obs}}^I D/\bar{v}^2)$, where \bar{v} is the average flow velocity in the tube. If the quantity $k_{\text{obs}}^I D/\bar{v}^2 \ll 1$, the effect is negligible. Under typical conditions, $k_{\text{obs}}^I \leq 10 \text{ sec}^{-1}$, $D \sim 100 \text{ to } 200 \text{ cm}^2 \text{ sec}^{-1}$, $\bar{v} \sim 500 \text{ cm/sec}$, the above quantity is ≤ 0.01 . The assumption of simple, one-dimensional plug flow, $\frac{d}{dt} = \bar{v} \frac{d}{dx}$, is therefore justified.

The second problem, perturbation by the probe, can be estimated by the approximate expression²¹

$$\ln \left(1 - \frac{c'}{c} \right) = - \left(\bar{v}^2 + 4 k^I D \right)^{1/2} \frac{x}{D}$$

where c' is the actual concentration x cm upstream of the probe and c is the hypothetical unperturbed concentration in the absence of the probe. Substitution of experimental parameters shows that for $x \geq 2$ cm the perturbation was $\leq 1\%$ so that probe effects could also be neglected.

D. Surface Recombination

Through proper selection of system parameters and by operating under conditions of negligible pressure drop, axial diffusion, and radial concentration gradients, the kinetic rate expression is reduced to

$$- \bar{v} \frac{d[H]}{dx} = k_w [H] + 2 k_M [H]^2 [M] \quad ,$$

i.e. the sum of the first order wall loss and the homogeneous term. Here we assume that recombination with $M = H$ can be neglected, since under most of our experimental conditions $[H] \leq 1\%$ and recent estimates¹² indicate that $k_R^H/k_R^{H_2} \leq 2$ near 300°K .

The relative importance of these remaining terms has been the subject

of some debate, and failure to include correction for possibly large wall losses has led to serious error in reported rate constants. In our system, the surfaces of the downstream dissociation and the cylindrical flow tube were poisoned with syrupy phosphoric acid and pumped until the residual flow of volatile species due to evaporation was less than 10^{-7} of the total flow under typical experimental conditions. Phosphoric acid has often been used for reducing surface loss and the values we obtained for the surface recombination coefficient were measured repeatedly and found to be between 10^{-5} and 10^{-6} . In order to measure the first order wall loss, one should operate under conditions where the wall loss term is greater than its homogeneous counterpart, i.e. where

$$k_{\text{wall}} > 2k_M [\text{H}] [\text{M}]$$

At 0.3 torr and $[\text{H}] \sim 8 \times 10^{13}$ atoms/cc, the pseudo first order term due to homogeneous recombination is reduced to about 0.01 sec^{-1} and the loss due to heterogeneous reaction can be measured directly. However, in these experiments, the above mentioned corrections for axial diffusion and probe perturbation must be applied. Experiments performed over a period of several years showed the wall loss to be small and easily controllable. Only infrequent recoating was required and the catalytic efficiency of the newly coated wall could be reduced through continued exposure to H/H₂ flows. The following is a chronological room temperature evaluation of k_w for a freshly poisoned surface measured over a period of 8 days: $k_w = 0.81, 0.80, 0.67, 0.42, 0.43, 0.39, \text{ and } 0.20 \text{ sec}^{-1}$. The value then leveled off and typically was found to be about 0.15 sec^{-1} corresponding to a surface recombination coefficient of 1.7×10^{-6} .

Under experimental conditions established to measure the homogeneous reaction rate constant, i.e. pressures greater than 5 torr, $[\text{H}] \geq 9 \times 10^{14}$ atoms/cc,

the heterogeneous loss contributed typically 3% to the observed falloff and the values for k_R were adjusted accordingly. Prior to our preliminary publication of some of the present results,²⁵ k_w had been estimated less accurately from experiments at several torr pressure, and assumed to be totally negligible. The small differences between $k_R^{H_2}$ values reported here and earlier²⁵ is entirely due to the subsequent subtraction of the small k_w term.

The behavior of k_w and probe efficiency at temperatures below 298°K is of considerable importance. As the NOCl titrations could not be carried out at 77°K, another method had to be used to check on the consistency of probe detection efficiency at low temperatures. Under conditions of constant H_2 and H-atom flow and of negligible reaction loss due to either homogeneous or heterogeneous recombination, the atom flux was measured at 298°K and the tube was then cooled to 77°K. No change was observed indicating constant detection efficiency. Also, experimental measurements of k_w at lower temperature showed it to be as small as or perhaps slightly smaller than its value at room temperature. Since k_R more than doubles as T decreases from 298 to 77°K, the correction due to heterogeneous reaction decreases to about 2% at 77°K.

E. Typical Kinetic Experiment

As in earlier studies involving catalytic probes,²¹ a voltage signal, simply related to the electrical power required to keep the probe at its preselected resistance (i.e. temperature), is obtained as a function of distance; and two such voltage vs. x traverses, one with atoms off and the other one with atoms on, provide an [H] vs. x (and thereby vs. t) scan. Our mechanical drive technique, coupled with the self-balancing Kelvin bridge, allows us to obtain a complete, continuous [H] vs. x scan in a few minutes, whereas earlier investigators positioned their detector point by point along

the flow tube and had to wait at each position for full thermal equilibration of the heated detector with its immediate surroundings. In the present arrangement, local heating effects cancel, because the probe, which is automatically held at constant temperature (normally 20 to 50° above ambient), is moved uniformly along the tube and thereby represents a local perturbation of the tube which is constant in time. This cancellation of potential errors was repeatedly confirmed by showing that [H] vs. x plots were independent of probe speed.

A typical set of x-y recorder traces, one each with atoms off and on, is shown in Fig. 7 and reveals the following interesting features: A rise in signal at the downstream position (near x = 0) due to local heating by the stationary probe near its starting position, because space limitations made it impossible to retract the probe farther downstream. As the probe moves upstream, away from its slightly heated initial position, the signal rises because more electrical power is required to keep it at its preselected resistance (temperature); a "dip" near 50 cm, which was entirely reproducible, corresponded to a rotation of the probe due to twisting of the long lead wires at the extreme downstream end of the flow tube extension. As it was present equally in both the atoms off and on runs at the same tube position, it had no effect on [H] vs. x plots.

Making use of the results of Sections III A, B, and C, we obtain the following expression for [H] from the measured difference in electrical power between atoms off and atoms on at any point along the flow tube:

$$[H] \text{ (atoms cm}^{-3}\text{)} = \frac{6.02 \times 10^{23} \times p \text{ (torr)}}{4.184 \times 760 \times \Delta H \times F \left(\frac{\text{cm}^3 \text{ atm}}{\text{sec}} \right)} \left(\frac{100 R_S}{100 + R_S} \right)^2 \frac{V_{\text{off}}^2 - V_{\text{on}}^2}{R_S}$$

where $\Delta H = 52.1$ kcal/gatom H, R_S (ohms) is the preselected resistance, normally near 2.5 ohms, and the V's (volts) are the voltages across the 1 ohm resistor

as read off plots such as Fig. 7. The results of Section III D further suggest that data analysis can proceed by simple $1/[H]$ vs. x plots, and that the corrected specific rate constant, k_R^M , can be calculated from the uncorrected $k_{unc} = \frac{\text{slope } \bar{v}}{2 [M]}$, as obtained in Fig. 8, by subtracting a small pseudo-third-order wall correction term, $k'_W = \frac{k_W}{2 [M] [H]_{av}}$, where $[H]_{av}$ is the average value of $[H]$ for that experiment. Although this last correction term artificially and wrongly expresses surface recombination as an equivalent third-order reaction, such a procedure is justified because k'_W is never larger than about 5% of k_{unc} and the rigorous computer analysis of such data using simultaneous first and second-order (third-order with $[M]$ constant) terms would be unnecessarily awkward and time-consuming. Typically, for experiments in pure H_2 at $298^\circ K$ and 6 torr with 1% H and a factor of two decrease of $[H]$ along the tube, $[H]_{av} \sim 1.5 \times 10^{15} \text{ cm}^{-3}$, and with $k_W \sim 0.15 \text{ sec}^{-1}$, $k'_W \sim 0.25 \times 10^{-33} \text{ cm}^6 \text{ sec}^{-1}$ or about 3% of measured $k_{unc} \sim 8.3 \times 10^{-33} \text{ cm}^6 \text{ sec}^{-1}$.

IV. Results and Discussion

A. $k_R^{H_2}$ at $296^\circ K$; Precision and Accuracy

The measurement of the $H + H + H_2$ rate constant at $296^\circ K$ was first carried out over a wide range of pressures (~ 2 to 15 torr), %H (0.2 to 4.7) and flow velocities (200 to 1300 cm/sec) to obtain a consistent and reliable value and to establish the kinetics of the process as clearly second-order in $[H]$ and first-order in $[H_2]$. Although $[H]$ decreased by only a factor of 2 to 3 in a typical experiment (Fig. 8), which is insufficient to prove second-order behavior, the constancy of the second-order rate constant at constant $[H_2]$ for widely different $[H]_0$, together with precisely linear $1/[H]$ vs. x plots proved the $[H]^2$ dependence of the rate. The linear $[H_2]$ dependence of the rate is shown in Fig. 9 in which the corrected second-order rate constants of 37 experiments at 2 to 15 torr are plotted vs. $[H_2]$. The slope of the

straight line plot is $8.0 \pm (\sigma = 0.2) \times 10^{-33} \text{ cm}^6 \text{ sec}^{-1}$, in excellent agreement with a value of $8.1 \pm 0.4 \times 10^{-33}$ for 73 experiments at 5 to 7 torr at 0.2 to 1.1% H. The continual verification of this rate constant was then used as a secondary standard in experiments at different temperatures, with different M-gases, and with D₂ in place of H₂, over a period of three years during which the probe was replaced once, the dissociator several times, the tube was re-coated several times, and flowmeters and transducers were replaced and recalibrated. Serious deviations from the above value of $k_R^{\text{H}_2}$ invariably led to the discovery of an experimental malfunction such as a leak or incomplete atom recombination on the probe (which was heated to dull redness in an H-atom stream at regular intervals). In all, about 200 such experiments were performed over a period of three years. They can be grouped as follows: ~ 100 runs (early work, T dependence, some D₂ work) -- $8.1 \pm 0.4 \times 10^{-33} \text{ cm}^6 \text{ sec}^{-1}$; 25 runs (mainly M = He work) - 8.1 ± 0.3 ; 31 runs (mainly M = Ar work) - 8.3 ± 0.3 ; 22 runs (new detector) - 8.1 ± 0.5 . An overall value of $8.1 \pm 0.4 \times 10^{-33} \text{ cm}^6 \text{ sec}^{-1}$ seems fully established where the 5% uncertainty equals a single standard deviation from the mean. It is difficult to estimate the contribution of systematic errors arising from the absolute accuracy of pressure and flowrate measurements, of flow tube dimensions, and of electrical components and meters. If these add an uncertainty of about 8%, we may estimate a total standard deviation of $\pm 10\%$. As a flowtube atom reaction rate measurement it appears to be one of the most precise and accurate.

B. Results for $k_R^{\text{H}_2}$ at $T < 298^\circ\text{K}$ and for k_R^{He} and k_R^{Ar} at 77° and 298°K .

Experimental results at 10 temperatures below 298°K are summarized in Table 2. Each set of low temperature data took about one day to collect and was nested between check runs at 298°K . Temperature equilibration at 77°K

was far more easily achieved than at intermediate temperatures where it required a stable balance between liquid nitrogen cooling rates and thermal losses. In achieving the flat, constant T vs. x profiles in the flow tube which are a prerequisite to a successful kinetic run, the catalytic probe was used as a sensitive, scanning resistance thermometer (with the atom source off) and T profiles were recorded (at ≥ 5 minute intervals to dissipate the effect of probe heating) until they were sufficiently constant in both x and t . The large number of experiments at 77°K reflects the ease of attaining that temperature as well as the need of collecting $k_R^{\text{H}_2}$ data at 77°K whenever k_R^{He} or k_R^{Ar} data were collected at that temperature.

Experiments with $M = \text{He}$ or Ar performed with those gases added either upstream or downstream of the dissociator gave identical results. In any series of runs, data were collected for pure H_2 and for anywhere from two to six different mole fractions of He or Ar , X_M , between 0 and 0.95. On the reasonable assumption that the measure rate constant, $k^T = X_{\text{H}_2} k^{\text{H}_2} + X_M k^M$, the extrapolated linear k^T vs. X_M plot gives k^M at $X_M = 1$. Such a plot for $M = \text{He}$ at 298°K is shown in Fig. 10. Assuming that errors may be slightly correlated in time, each series of X_M runs was analyzed to obtain a k^M/k^{H_2} ratio and these ratios were averaged as shown in the first two columns of Table 3. The ratios were then multiplied by the best, averaged k^{H_2} at that temperature to give k^M as shown in the last two columns. k^{He} is seen to be $13 \pm 6\%$ smaller than k^{H_2} at 298° and $35 \pm 9\%$ smaller at 77°K whereas k^{Ar} is $14 \pm 9\%$ larger than k^{H_2} at 298° and $48 \pm 30\%$ larger at 77°K which indicates an increasing temperature dependence from He to H_2 to Ar .

C. Deuterium Atom Recombination at 77° and 298°K .

Measurements of the $\text{D} + \text{D} + \text{D}_2$ rate constant were straight-forward and entirely analogous to their H counterparts, but the high cost of D_2 made

it necessary to use H_2 for all initial conditioning including check runs of k^{H_2} and k_W , then to switch to D_2 at low flowrates for about 20 minutes, then to measure k_W for D-atoms at low pressure, and finally to collect data for the homogeneous recombination at 4 to 10 torr. k_W was found to be about equal to its value for H-atoms, but since $k_R^{D_2}$ is 25% smaller than $k_R^{H_2}$, the surface correction term was 5%, slightly larger than for its H_2 counterpart. More than 30 experiments at 298°K gave $k_R^{D_2} = 6.1 \pm 0.3 \times 10^{-33} \text{ cm}^6 \text{ sec}^{-1}$ or a k^{D_2}/k^{H_2} ratio of 0.75 ± 0.05 . The result of 8 experiments at 77°K was $15.1 \pm 1.0 \times 10^{-33} \text{ cm}^6 \text{ sec}^{-1}$ or a k^{D_2}/k^{H_2} ratio of 0.82 ± 0.11 .

D. Comparison with Earlier Experimental Results.

Although much of the early work, especially that of the 1930's, was carefully done, experimental conditions were such that it is impossible to unravel the contributions to the observed kinetics due to surface recombination, thermal effects, and M-effects (particularly for large $[H]/[H_2]$). This leaves only the work of Larkin and Thrush^{10,11} and that of Bennett and Blackmore¹²⁻¹⁴ for comparison. For $M = H_2$, Larkin and Thrush reported $9.4 \pm 1.4 \times 10^{-33} \text{ cm}^6/\text{sec}$ at 293°K ($9.3 \pm 1.4 \times 10^{-33}$ at 298°K) which is in satisfactory agreement with our $8.1 \pm 0.4 \times 10^{-33}$. Bennett and Blackmore first reported¹² $3.7 \pm 0.5 \times 10^{-33}$ in a clean quartz tube at 2 to 9 Torr pressure, then $4.7 \pm 0.7 \times 10^{-33}$ at 50 to 250 torr in the quartz tube¹³, and finally $5.8 \pm 0.7 \times 10^{-33}$ at 1.4 to 5.9 torr in a Teflon-coated flow tube.¹⁴ Surface recombination was taken into account in all three studies. Moreover, these authors found a strong negative correlation of k_R with k_W , an effect never encountered by us. The upward trend of k_R amounts to 57% going from ref. 12 to 14, yet is termed 'good agreement', but seems puzzling as do two other observations: (1) the unusually large degree of dissociation of highly purified H_2 in microwave discharges reported in

ref. 12 which runs counter to the experience of several other groups and suggests that the electron spin resonance measurements substantially over-estimated $[H]$ in these experiments and that k_R was therefore too low; (2) the $k_R^{D, D_2} / k_R^{H, H_2}$ ratio of 1.3, in substantial disagreement with our 0.75 and with theory.^{26, 27}

Poor agreement also abounds for M-effect at 298°K. For $k_R^{He} / k_R^{H_2}$ Bennett and Blackmore¹³ report 1.3 compared to our 0.87. For $k_R^{Ar} / k_R^{H_2}$ they find 1.7, Larkin and Thrush¹⁰ 0.66, and we 1.14. The Bennett and Blackmore M-data¹³ refer to their high pressure flow tube experiments whose interpretation in one dimensional plug flow using the average flow velocity and neglecting the parabolic velocity distribution as well as the slow radial diffusion probably introduces large errors as Poirier and Carr's²⁸ analysis suggests.

Only Larkin and Thrush¹⁰ report some temperature dependence results near 300°K. Expressed in T^{-n} form, their data at 213, 293, and 349°K give $n = 0.68$, in satisfactory agreement with $n = 0.81$ based on our k_R^{Ar} values at 77 and 298°. A similar, empirical fit of our two k_R^{He} points gives $n = 0.40$ and a weighted least squares fit to all of our $k_R^{H_2}$ data of Table 2, except for the $T = 77^\circ K$ point which falls below the good straight line on a log-log plot, gives $n = 0.68$. Two point fits of $k_R^{H_2}$ using only 77 and 298° and of $k_R^{D_2}$ give 0.61 and 0.67, respectively.

E. Comparison with Theory

It has been the multiple curse laid on our detailed understanding of atom recombination processes in general, and that of H in particular, that a variety of simple-minded models of the process give a very reasonable account of the magnitude of the rate constant in zero order approximation, but that very little improvement is achieved when the models are refined

and are then expected to describe the process in detail. Moreover, the experiments are difficult and the total range of the quantity, k_R , whose dependence on T and on M forms the principal criterion on which the models are evaluated, is very small, indeed. Thus, in the present work a factor of four temperature change produces only 1.7 to 3 fold changes in k_R , and M-effect ratios range from a minimum of 0.65 to a maximum of 1.48, whereas a single standard deviation of a given k_R may be 5 to 15% and that of ratios 7 to 20%. Considering these limitations it is surprising how much indirect information can be extracted from the present data.

The principal questions are as follows: A. Is it possible to determine if and to what extent a given $H + H + M$ recombination proceeds via the energy transfer (ET) mechanism, the radical-molecule-complex (RMC) mechanism, or both? B. For the H-atom recombination at low temperature ($\leq 300^\circ K$) can it be shown whether the process proceeds principally via orbiting resonances of H_2 (and HM), i.e. by quantum mechanical tunneling through the rotational barrier? If these questions can be answered, one may then hope to extract from the data some information on the interatomic potentials.

Benson and Fueno²⁹ calculated k_R^{Ar} in the ET approximation using a steady-state stepladder model with either Morse or Lennard-Jones functions characterizing the vibrational states near the dissociation continuum. In magnitude, their Lennard-Jones results of 1.00 or $1.05 \times 10^{-32} \text{ cm}^6 \text{ sec}^{-1}$ (depending on whether gas kinetic or Sutherland deactivation cross sections are used) are much closer to the experimental 0.92×10^{-32} than their Morse results of 5.0 or 3.7×10^{-32} , but neither model comes close to giving the correct temperature dependence as they give $n < 0.2$.

Keck's classical variational phase space theory was recently applied to H-recombination by Shul and Appleton²⁰ (SA). The orbiting resonance theory

was proposed by Roberts, Bernstein, and Curtiss¹⁸ (RBC), recently modified by Whitlock, Muckerman, and Roberts³⁰ (WMR), and extended to include contributions by the RMC mechanism by Pack, Snow, and Smith³¹ (PSS). The comparison of our data with these theories is shown in Figs. 11 ($M=H_2$), 12 ($M=He$), and 13 ($M=Ar$). It is best, in posing questions A and B to examine all three figures simultaneously. The original orbiting resonance theory¹⁸ (RBC) predicts the correct magnitude of k_R^M to better than a factor of two, but shows much too small a temperature dependence due to its following shortcomings: (1) Too crude a model for the calculation of rotational relaxation cross sections, e.g. assuming metastable H_2^* to be a rigid rotor; (2) Neglect of the RMC mechanism which could lead to underestimates of k_R^{Ar} and of all k_R^M at the lowest temperature; (3) Neglect of metastable, non-resonant states of H_2 and of free states with energy above the rotational barrier; (4) Neglect of departures from equilibrium. Correction of (1) above was made by WMR for $M = H_2$ using classical trajectory calculations. This produced improvement but still predicted too flat a T-dependence at low temperature. A second calculation by WMR, not shown in Fig. 11, followed SA and PSS in using an attractive H - H_2 potential with a 38°K well depth (whereas the WMR curve in Fig. 1 had used a repulsive H - H_2 potential) to calculate the $H_2^* - H_2$ relaxation cross section. It duplicated the shape of the experimental curve, but is everywhere too high by about 20 to 40%. The classical SA calculation also reproduces the shape of the $k_R^{H_2}$ vs. T curve, but falls 20 to 30% below the experimental points even though it contains a substantial contribution from the RMC mechanism and uses an H - H_2 potential which is probably too strongly attractive. If the potential proposed by Dalgarno, Henry, and Roberts³², which supports no bound levels ($\epsilon/k = 15^\circ K$), is correct, much of the RMC contribution would have to be removed and both the magnitude of the SA rate constant and its

temperature dependence would then be incorrect. Low energy ($\sim 20^\circ\text{K}$) beam scattering experiments on $\text{H} + \text{H}_2$ would be particularly welcome, since data which are presently becoming available³³ are in too high an energy range to probe the depth and shape of the potential well. The PSS calculation extends the RBC theory by including the contribution which M-H resonances make to the recombination, i.e. by including the quantum mechanical RMC mechanism, and by evaluating the inelastic collision cross sections in the WKB approximation. For $M = \text{H}_2$, these calculations overestimate k_R somewhat near 300°K and underestimate it at 77°K even though they use the deep (38°K) attractive well for $\text{H}-\text{H}_2$. It is interesting to note that the addition of the RMC contribution (as indicated separately in the PSS paper but not in Fig. 11) to the WMR rate constant would produce good agreement with our experimental values over the entire temperature range (but less so if the $\text{H}-\text{H}_2$ potential has a shallower well).

For $M = \text{He}$, all theories predict a flatter k_R vs. T plot than the admittedly slim experimental evidence indicates. SA's phase space calculations are able to reproduce such a steeper dependence (not shown in Fig. 12) by using a well depth of 39°K , $r_e = 3.7\text{\AA}$, and $\beta = 1.87\text{\AA}^{-1}$ in the Morse potential for $\text{H}-\text{He}$. This probably is much too strong an interaction. Recent theoretical³⁴ and experimental³⁵ studies indicate a well depth in the 5 to 10°K range, in line with the now accurately measured $\text{He}-\text{He}$ well depth of $11.0 \pm 0.2^\circ\text{K}$ ³⁶. Such a potential does not support a bound $\text{H}-\text{He}$ state and removes the possibility of a RMC recombination pathway as shown by the flat maximum in k_R at 100 to 150°K calculated by PSS. The older RBC calculation comes closest to fitting the data, but in view of its approximations, this is probably not significant.

For $M = \text{Ar}$, all recent calculations fall below the experimental points and only the RBC curve has a maximum. PSS report a smaller RMC contri-

bution in the $M = \text{Ar}$ than in the $M = \text{H}_2$ case which is surprising, particularly since a sizable well depth of 47.7°K is used for $\text{H} - \text{Ar}$ ($r_e = 3.36\text{\AA}$). For a reasonable choice of potential, the classical SA curve has the correct shape, but again falls well below the experimental values.

The k_R^D/k_R^H ratio is in good agreement with both classical and quantum calculations. The latter²⁷ also predict an increase of this ratio with decreasing temperature which is marginally supported by our observed rise from 0.75 ± 0.05 to 0.81 ± 0.11 .

To return to the questions posed earlier: it seems that the $M = \text{Ar}$ data and the $M = \text{H}_2$ results at the lowest temperatures are not easily rationalized without appeal to the RMC mechanism, but that it plays a minor role under all conditions investigated here except, perhaps, for $M = \text{Ar}$ near 77°K . It would be desirable, therefore, to extend recombination rate measurements to still lower temperatures, particularly for $M = \text{He}$.

On the question of quantum vs. classical models a clear decision can not be made. The resonance theory is physically more reasonable and has shown good agreement with experiment at an earlier stage in its development, i.e. with less refinement and for more realistic choices of interaction potentials. More rigorous calculations should be carried out to ascertain the role of non-resonant as well as continuum states as recombination intermediates. The present experimental work is continuing with measurement of other M-effects including, hopefully, $M = \text{H}$ and of the ortho-para ratio of recombined H_2 in an attempt to resolve question B directly³⁷.

REFERENCES

*Supported by the National Science Foundation under Grant #GP-10327

†Andrew Mellon Predoctoral Fellow. This work was submitted in partial fulfillment of the requirements for the degree of Doctor of Philosophy at the University of Pittsburgh. Present address: Avco Everett Research Laboratory, Everett, Massachusetts 02149.

††Present address: Department of Chemistry, University of Rochester, Rochester, New York 14627.

1. H. M. Smallwood, J. Am. Chem. Soc. 51, 1985 (1929); 56, 1542 (1934).
2. H. Senftleben and O. R. Riechemeier, Ann. Physik 6, 105 (1930);
H. Senftleben and W. Hein, *ibid* 22, 1 (1935).
3. W. Steiner and F. W. Wicke, Z. Physik. Chem. (Bodenstein Festband) 817 (1931); W. Steiner, Trans. Faraday Soc. 31, 623 (1935).
4. I. Amdur and A. L. Robinson, J. Am. Chem. Soc. 55, 1395 (1933);
I. Amdur, *ibid* 57, 856 (1935); 60, 2347 (1938).
5. L. Farkas and H. Sachsse, Z. Physik. Chem. B27, 111 (1934).
6. S. Shida, Proc. Imper. Acad. (Tokyo) 17, 495 (1941).
7. L. Avramenko and R. V. Kolesnikova, Izvest. Akad. Nauk. SSSR, Otd. Khim. Nauk., 1971(1961).
8. T. C. Marshall, Phys. Fluids 5, 743 (1962).
9. C. B. Kretschmer and H. L. Petersen, J. Chem. Phys. 39, 1772 (1963).

10. F. S. Larkin and B. A. Thrush, *Discussions Faraday Soc.* 37, 112 (1964); 10th Sympos. (Internatl.) on Combustion, The Combustion Institute, Pittsburgh, Pa. 1965, p. 397.
11. F. S. Larkin, *Can. J. Chem.* 46, 1005 (1968).
12. J. E. Bennett and D. R. Blackmore, *Proc. Roy. Soc.* A305, 553 (1968).
13. J. E. Bennett and D. R. Blackmore, 13th Sympos. (Internatl.) on Combustion, The Combustion Institute, Pittsburgh, Pa. 1971, p. 51.
14. J. E. Bennett and D. R. Blackmore, *J. Chem. Phys.* 53, 4400 (1970).
15. S. Miyazaki and S. Takahashi, *Mem. Def. Acad. Japan IX*, 643 (1969).
16. V. V. Azatyan, L. B. Romanovich, and S. B. Eilippov, *Kinet. Katal.* 9, 1188 (1968).
17. D. L. Baulch, D. D. Drysdale, D. G. Home, and A. C. Lloyd, *Evaluated Kinetic Data for High Temperature Reactions, Vol. I*,
18. R. E. Roberts, R. B. Bernstein, and C. F. Curtiss, *J. Chem. Phys.* 50, 5163 (1969).
19. V. H. Shui, J. P. Appleton, and J. C. Keck, *J. Chem. Phys.* 53, 2547 (1970).
20. V. H. Shui and J. P. Appleton, *J. Chem. Phys.* 55, 3126 (1971).
21. E. L. Tollefson and D. J. Leroy, *J. Chem. Phys.* 16, 1057 (1948); J. E. Morgan and H. I. Schiff, *ibid* 38, 2631 (1963); B. Khouw, J. E. Morgan, and H. I. Schiff, *ibid* 50, 66 (1969).
22. M. A. A. Clyne and B. A. Thrush, *Trans. Faraday Soc.* 57, 1305 (1961).
23. M. A. A. Clyne and D. H. Stedman, *Trans. Faraday Soc.* 62, 2164 (1966).
24. F. Kaufman, in *Progress in Reaction Kinetics*, G. Porter, Ed., London, Pergamon Press, Vol. I, p. 3.
25. D. O. Ham, D. W. Trainor, and F. Kaufman, *J. Chem. Phys.* 53, 4395 (1970).

26. T. A. Jacobs, R. R. Gledt, and N. Cohen, *J. Chem. Phys.* 48, 947 (1968).
27. R. E. Roberts and R. B. Bernstein, *Chem. Phys. Letters* 6, 282 (1970).
28. R. V. Poirier and R. W. Carr, Jr., *J. Phys. Chem.* 75, 1593 (1971).
29. S. W. Benson and T. Fueno, *J. Chem. Phys.* 36, 1597 (1962).
30. P. A. Whitlock, J. T. Muckerman, and R. E. Roberts, *Chem. Phys. Letters* 16, 460 (1972).
31. R. T. Pack, R. L. Snow, and W. D. Smith, *J. Chem. Phys.* 56, 926 (1972).
32. A. Dalgarno, R. J. W. Henry, and C. S. Roberts, *Proc. Phys. Soc. (London)* 88, 611 (1966).
33. C. Hahn, Dissertation, Born, 1972; R. W. Bickes, B. Lautzsch, J. P. Toennies, and K. Walaschewski, to be published.
34. G. Das and A. C. Wahl, *Phys. Rev. A* 4, 825 (1971).
35. R. Gengenbach, C. Hahn, and J. P. Toennies, *Phys. Rev. A*, in press.
36. P. E. Siska, J. M. Parson, T. P. Schafer, and Y. T. Lee, *J. Chem. Phys.* 55, 5762 (1971); J. M. Farrar and Y. T. Lee, *J. Chem. Phys.* 56, 5801 (1972).
37. R. E. Roberts, *J. Chem. Phys.* 54, 1422 (1971); M. Menzinger, *Chem. Phys. Letters* 10, 507 (1971).

Table 1

Comparison of [H] Measurement by NOC₂ Titration
and by Catalytic Probe

Total Pressure (Torr)	[H] (10 ¹⁵ atoms/cc)	[H] _{probe} (10 ¹⁵ atoms/cc)	[H] _{probe} /[H] (%)
2.12	0.86	0.80	93
1.29	1.32	1.17	89
2.22	1.28	1.19	93
1.30	1.29	1.26	97
1.00	1.27	1.28	101
1.34	1.25	1.32	106
1.35	1.59	1.48	93
1.35	1.34	1.49	111
1.94	1.54	1.58	103
1.95	1.51	1.63	<u>107</u>
		Mean Value	= 99 ± 8

Table 2

 $k_R^{H_2}$ as a Function of Temperature

Temperature (°K)	Number of Experiments	$k_R \times 10^{33}$ (cm ⁶ /sec) uncorrected for wall loss	$k_R \times 10^{33}$ (cm ⁶ /sec) corrected for wall loss
298	> 175	8.3 ± 0.4	8.1 ± 0.4
275	7	8.5 ± 0.5	8.3 ± 0.5
253	6	9.6 ± 0.3	9.4 ± 0.3
231	6	10.0 ± 0.8	9.8 ± 0.8
210	6	10.8 ± 0.9	10.5 ± 0.9
200	5	11.3 ± 0.2	11.1 ± 0.2
180	6	11.7 ± 0.2	11.4 ± 0.2
160	8	12.2 ± 1.0	12.0 ± 1.0
140	7	13.5 ± 0.9	13.3 ± 0.9
120	8	15.6 ± 1.6	15.4 ± 1.6
77	72	18.9 ± 2.2	18.5 ± 2.2

Table 3

Recombination Rate Constants, k_R^M , at 77 and 298°K

M	$k_R^M / k_R^{H_2}$		$k_R^M \times 10^{33}$ (cm ⁶ /sec)	
	298°K	77°K	298°K	77°K
H ₂	1.0	1.0	8.1 ± 0.4	18.5 ± 2.2
He	0.87 ± 0.06	0.65 ± 0.09	7.0 ± 0.4	12.0 ± 1.5
Ar	1.14 ± 0.09	1.48 ± 0.30	9.2 ± 0.6	27.4 ± 4.6
D ₂ (D)	0.75 ± 0.05	0.82 ± 0.11	6.1 ± 0.3	15.1 ± 1.0

LEGEND FOR FIGURES

- Fig. 1 Diagram of apparatus
- Fig. 2 H-atom source
- Fig. 3 Catalytic probe support
- Fig. 4 self-balancing Kelvin bridge
- Fig. 5 Probe collection efficiency determination
- Fig. 6 NOCl titration comparison
- Fig. 7 Typical recorder traces for measurement of [H] vs. x
- Fig. 8 $1/[H]$ vs. x plot
- Fig. 9 Plot of second order H-atom decay rate constant, k^{II} vs. P_{H_2}
- Fig. 10 Plot of total third order rate constant, k^T vs. X_{H_2}
- Fig. 11 $k_R^{H_2}$ vs. T. \square - this work; RBC - ref. 18; SA - ref. 20; WMR - ref. 30;
PSS - ref. 31
- Fig. 12 k_R^{He} vs. T. symbols as in Fig. 11
- Fig. 13 k_R^{Ar} vs. T. symbols as in Fig. 11; Δ - ref. 10

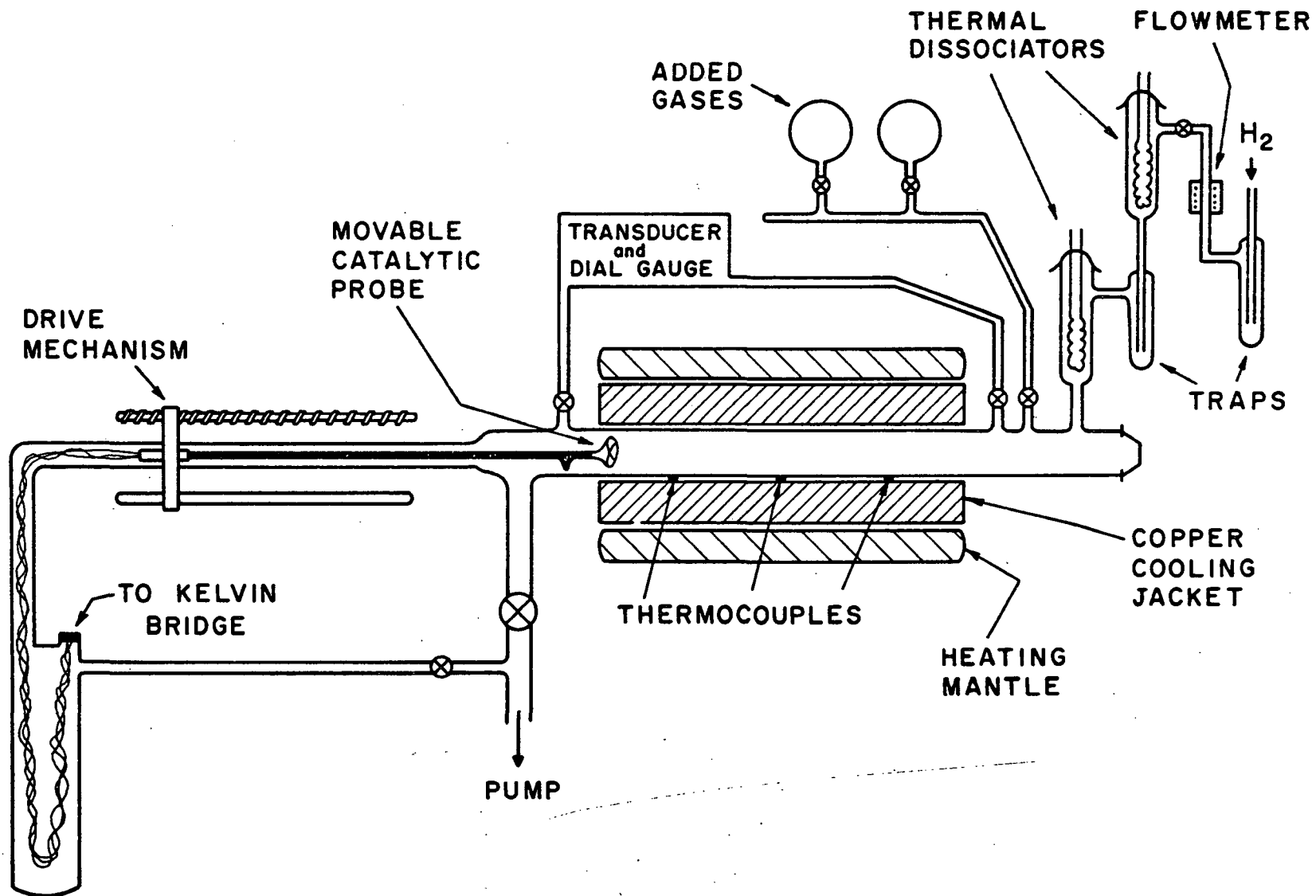


FIGURE 1

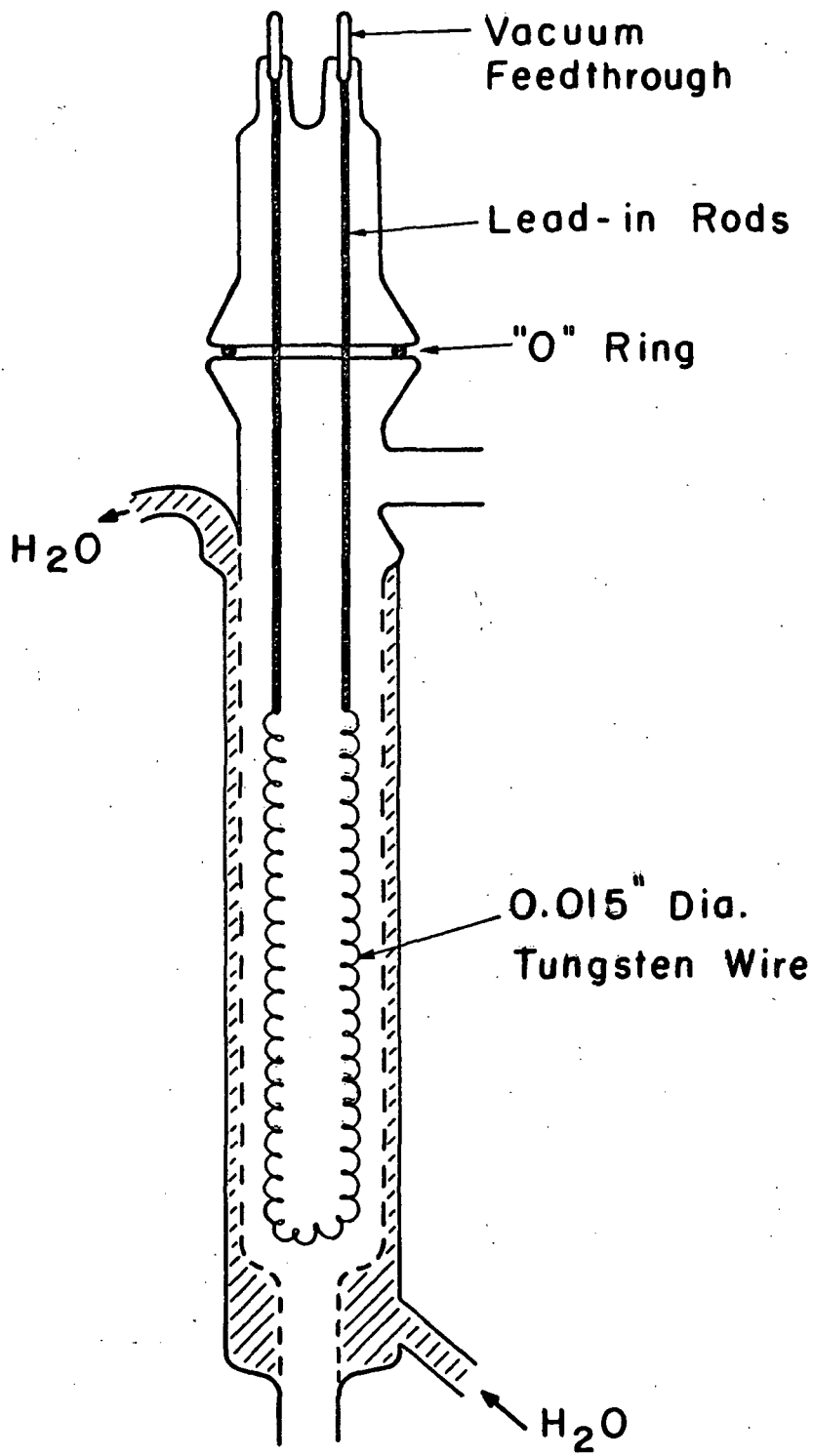


FIGURE 2.

CATALYTIC PROBE

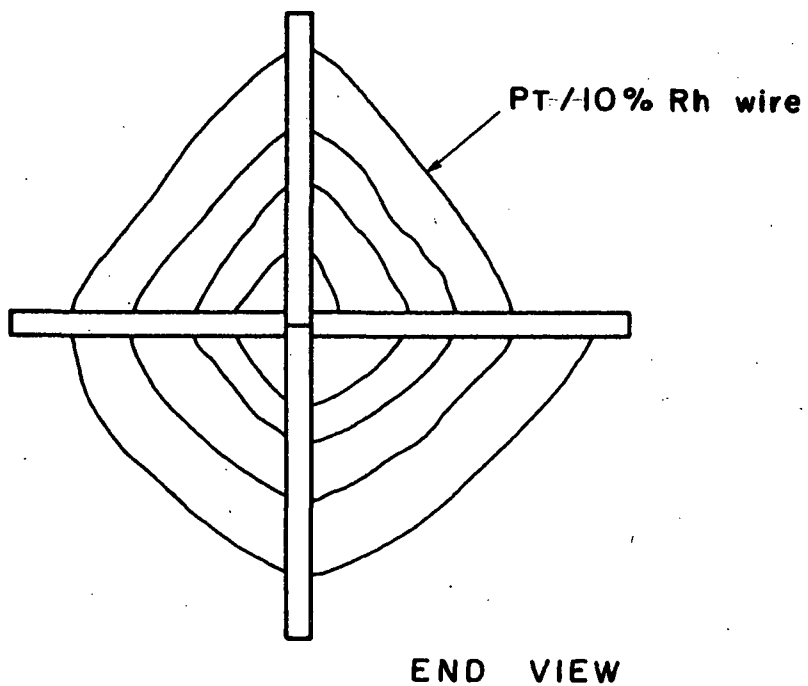
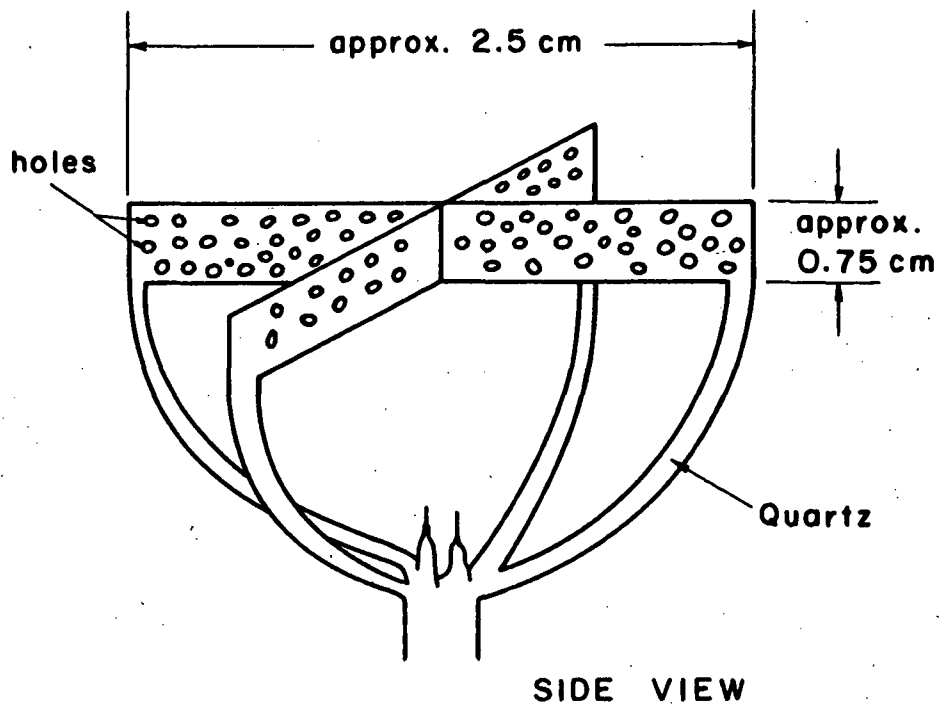


FIGURE 3

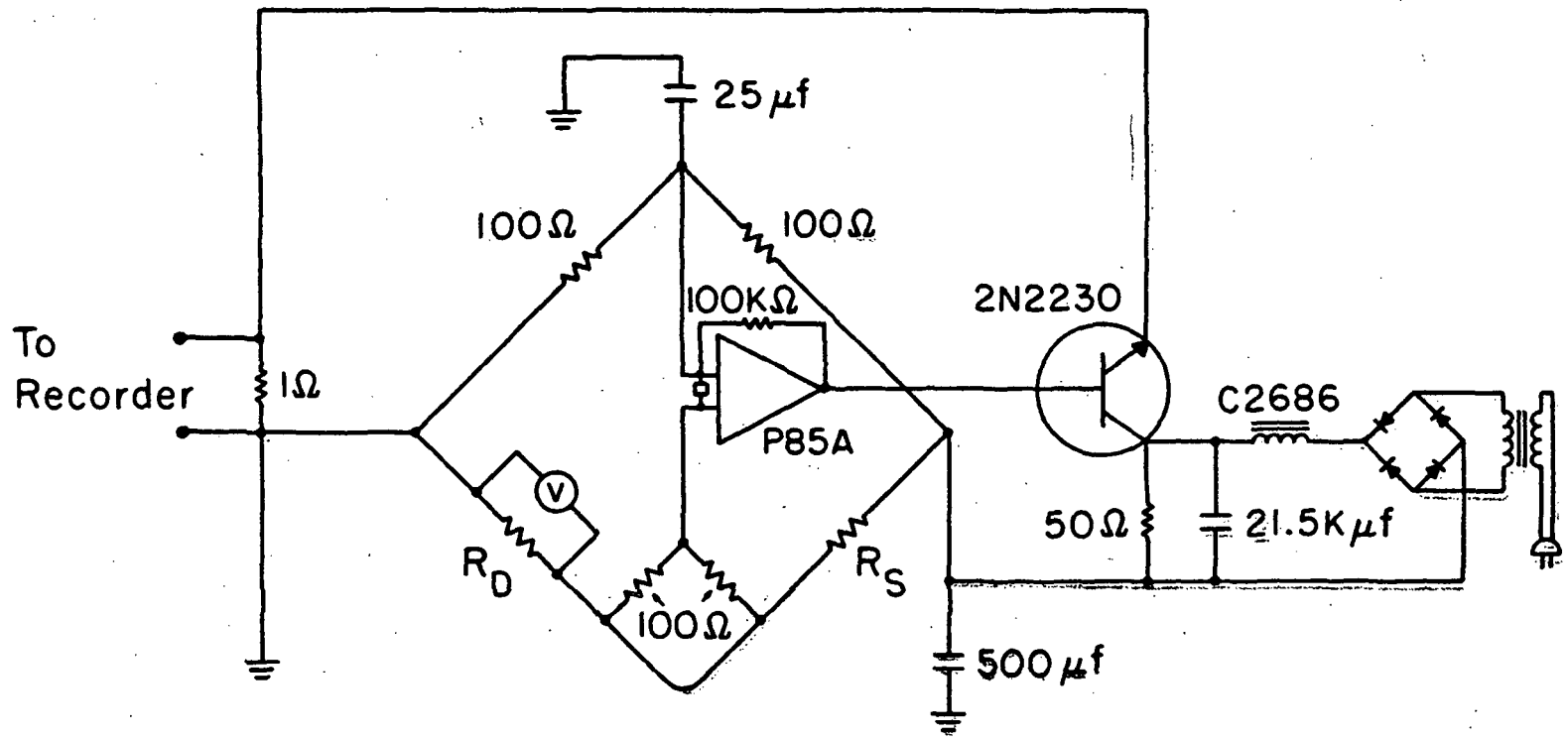


FIGURE 4

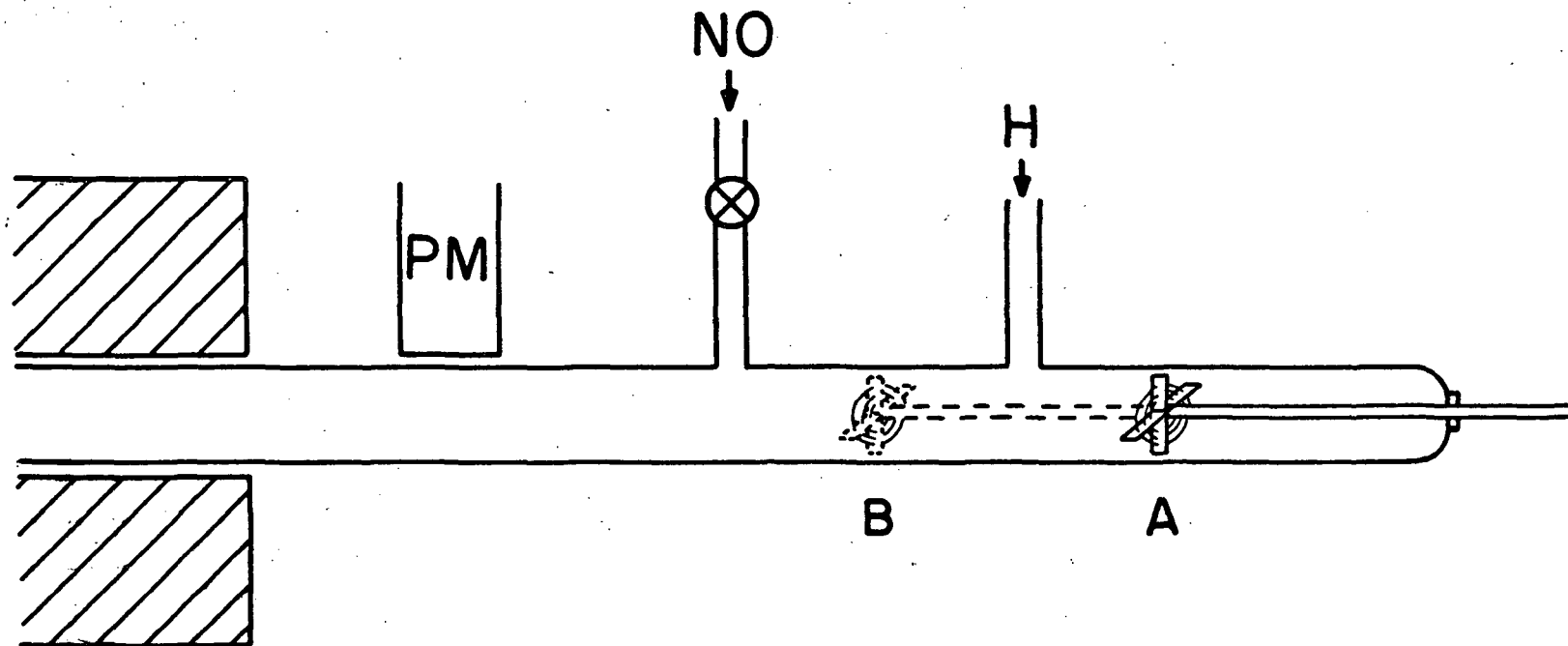


FIGURE 5

Intensity / [NOCl]_{added}

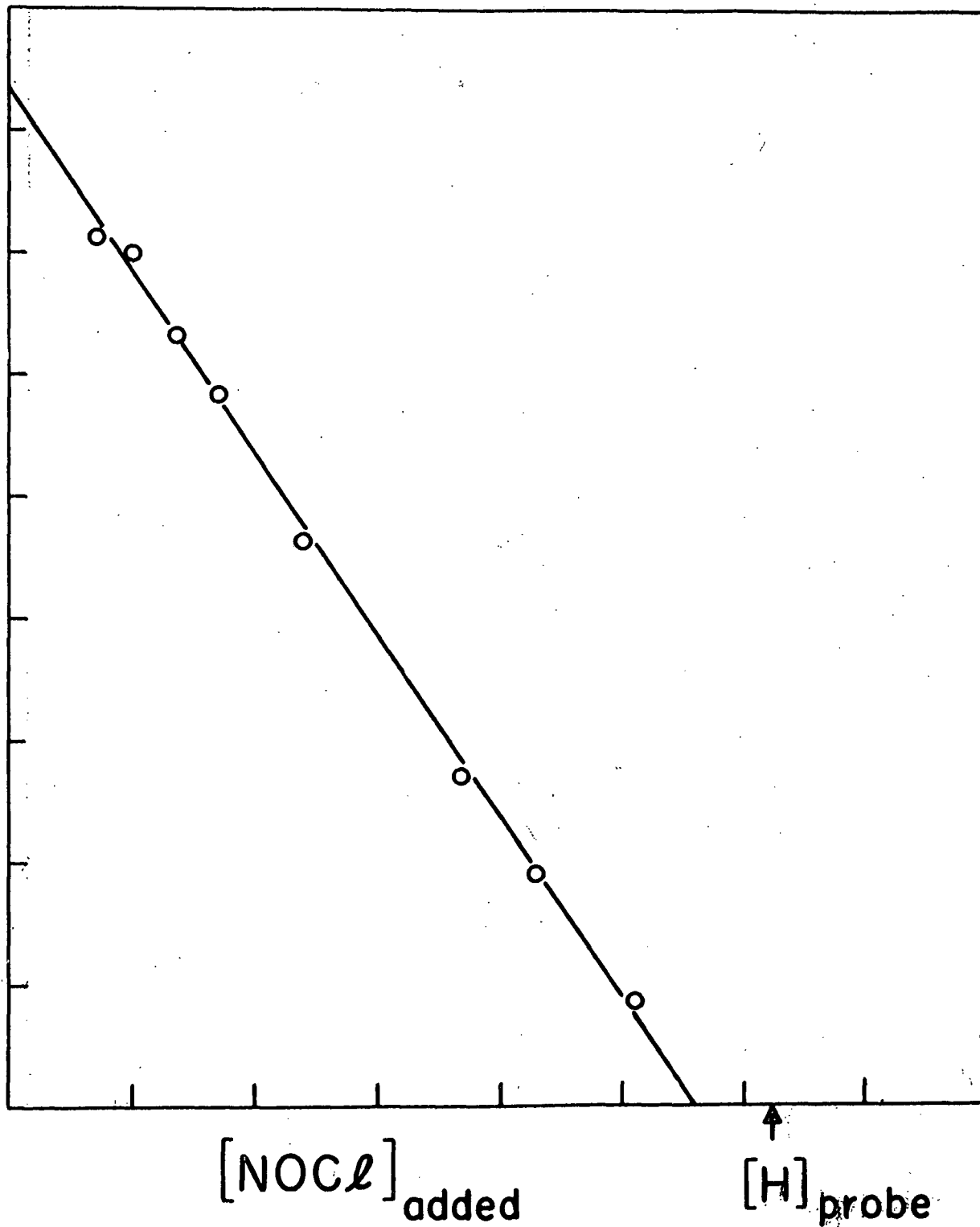


FIGURE 6

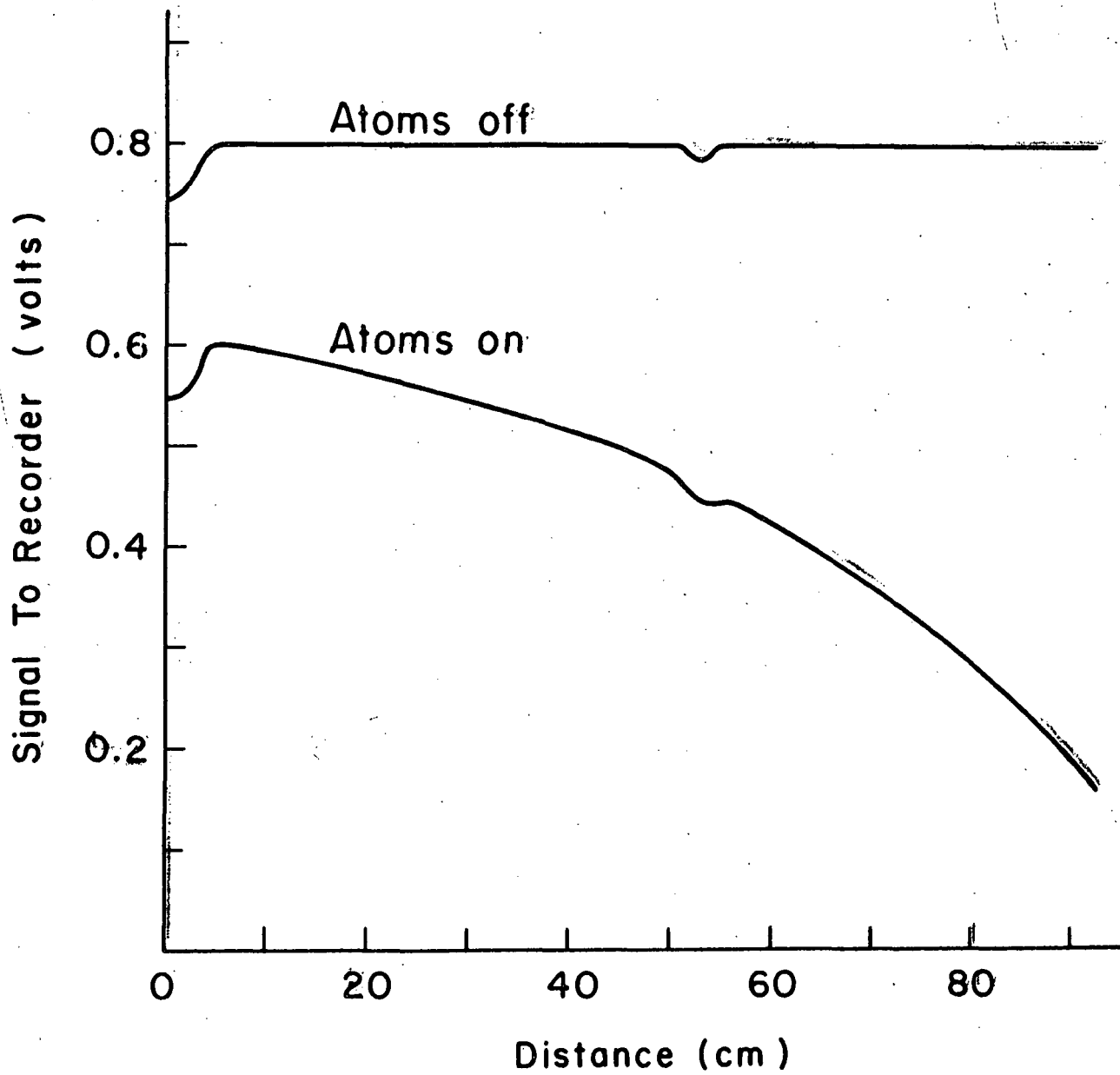


FIGURE 7

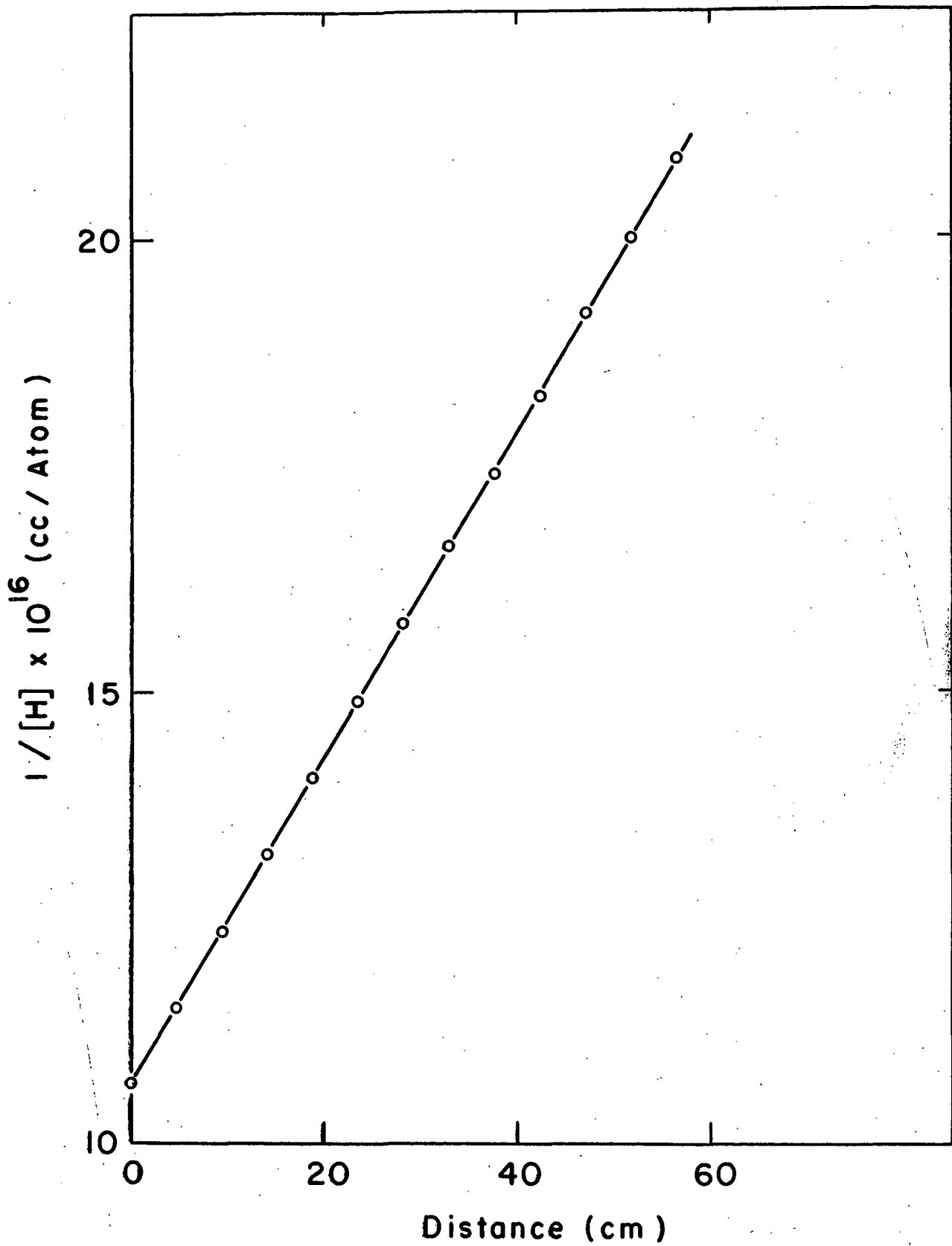


FIGURE 8

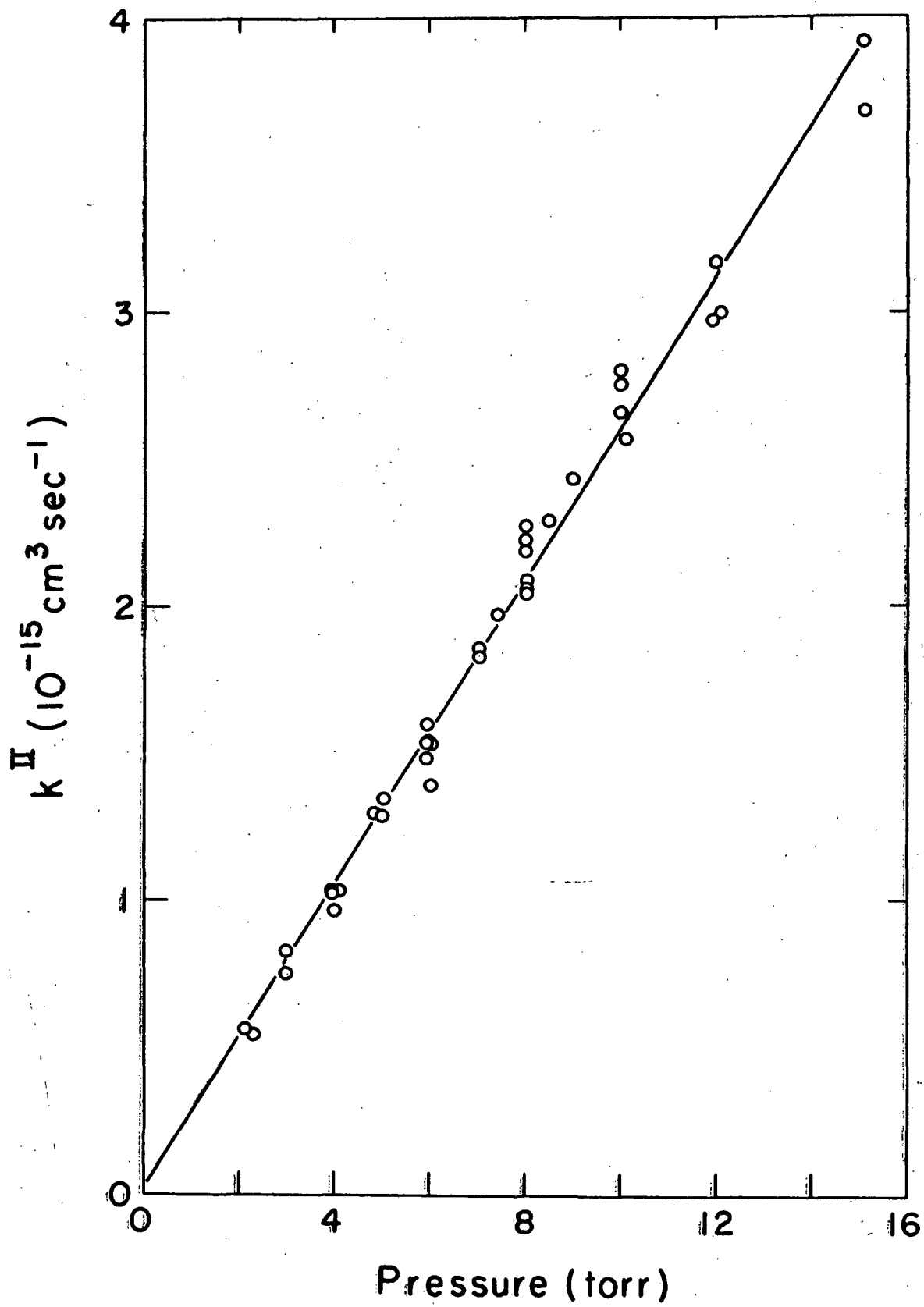


FIGURE 9

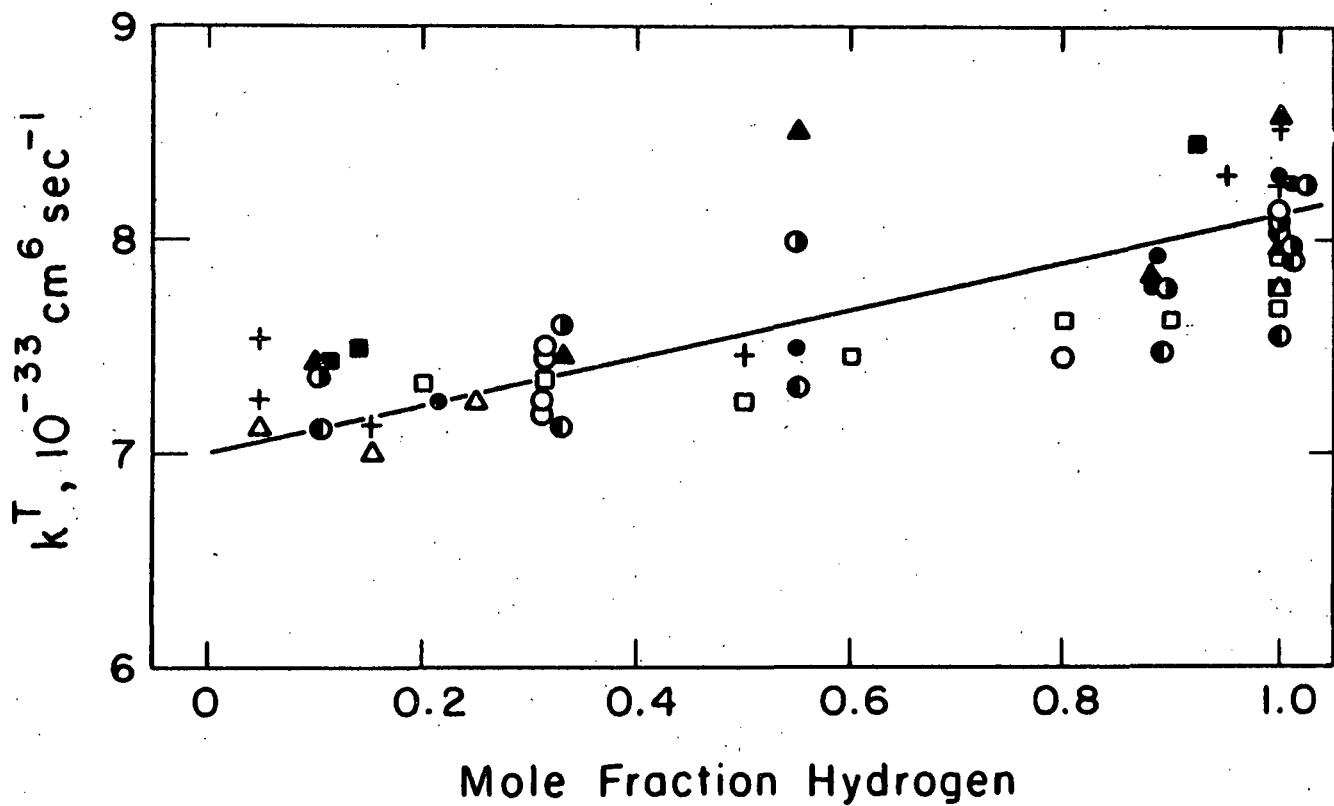


FIGURE 10

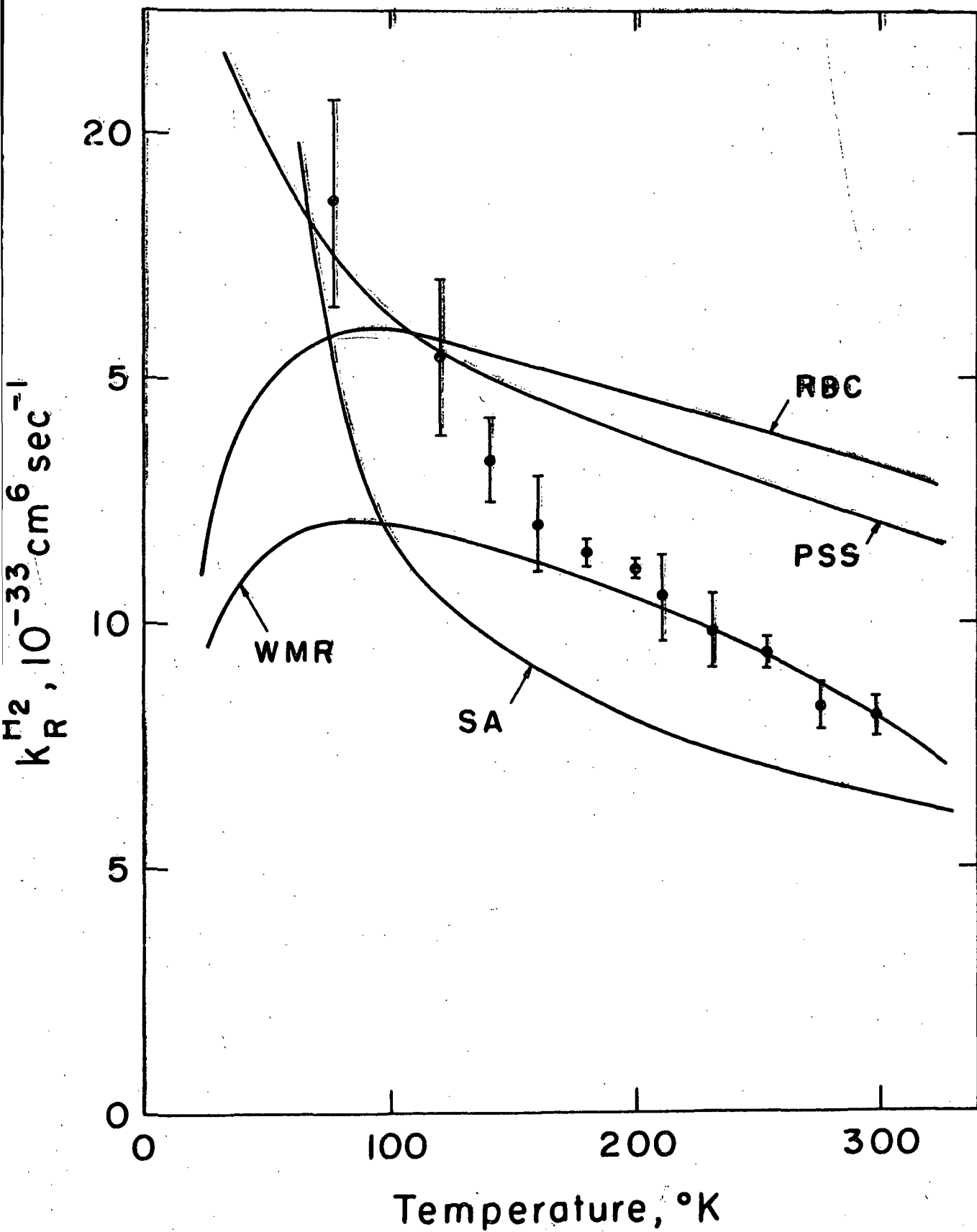


FIGURE 11

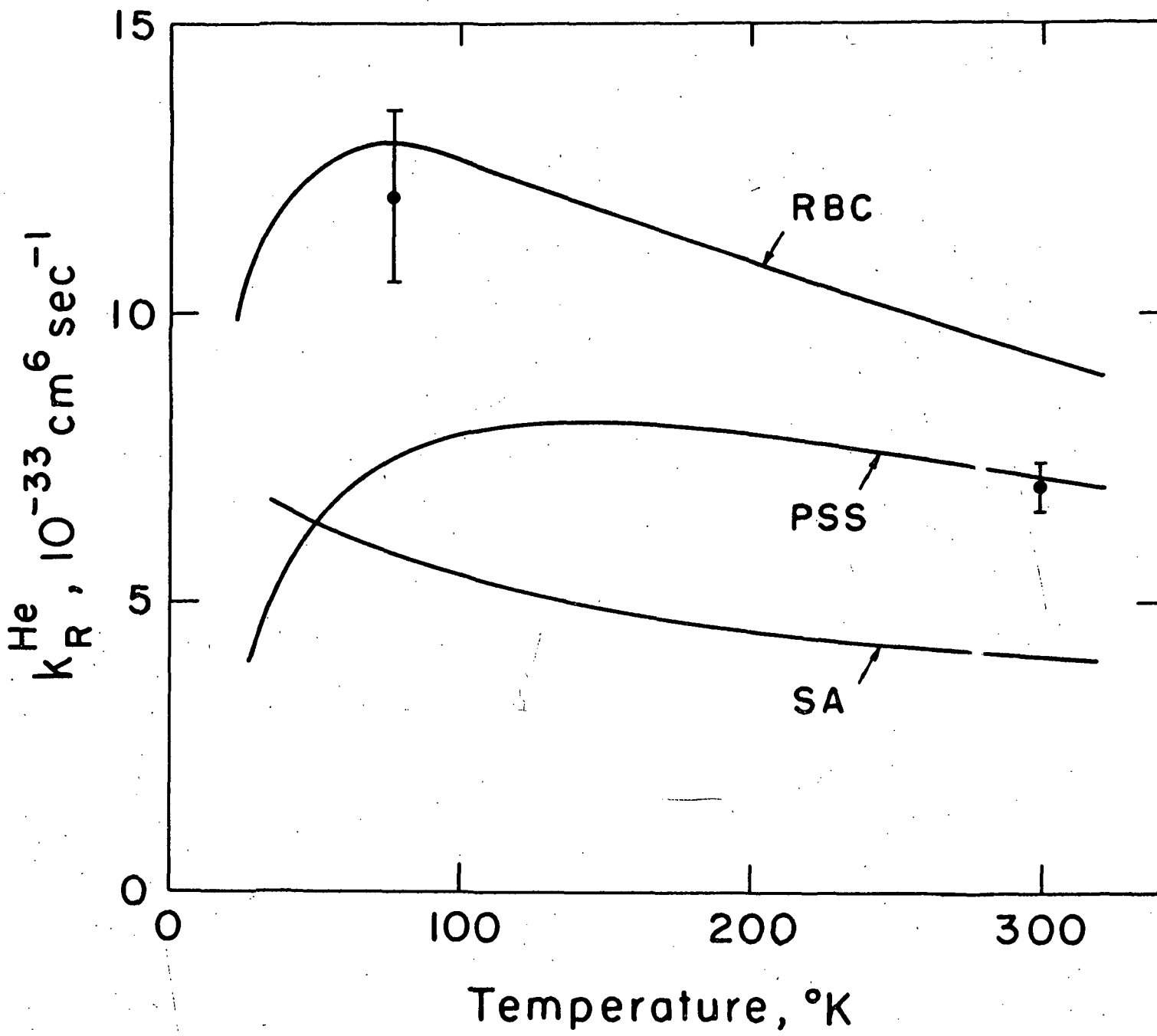


FIGURE 12

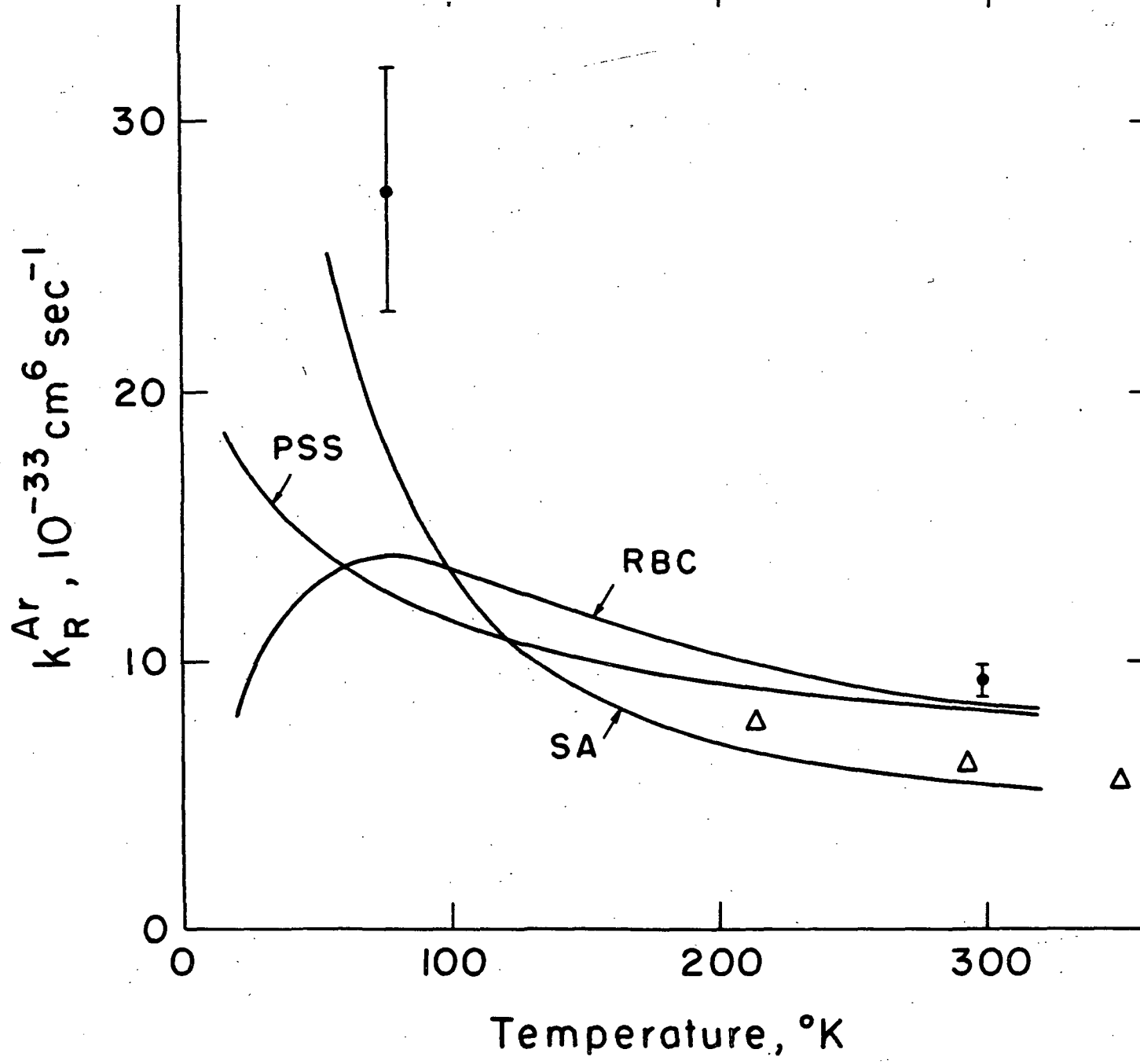


FIGURE 13